

Modified One Cycle Controlled Scheme for Single-Phase Grid Connected Pv-Fc Hybrid System

Sattineni Nagaprasad¹, Naveen Boliseti², P Ram Prasad³

^{1,3}Swarnandhra College of Engineering and Technology

²SRKR Engineering college

Abstract: AC to DC converters based on one cycle control exhibit instability in current control. In this paper modified one cycle control(MOOC) for bidirectional ac to dc is proposed. The sum of fictitious current and the actual load current is compared with a sawtooth waveform to generate the generating switches. In order to interface the inverter with the grid service of a phase locked loop(PLL) is required. Designing a phase locked loop for interfacing with a weak grid is always a difficult proposition considering the nonidealities like frequency variation and harmonic distortions in the line voltages. Renewable energy is currently widely used one of these resources is solar energy. The pv array normally uses a maximum power point tracking (MPPT) technique to continuously deliver the highest power to the load when there are variations in irradiation and temperature, making it an uncontrollable source. The disadvantage of pv energy is that the pv output power depends on weather conditions and cell temperature further it is not available during night. In order to overcome these drawbacks alternative source such as proton exchange membrane fuel cell (PEMFC) should be installed in the hybrid system by changing the fuel cell output power the hybrid sources output becomes controllable.

Keywords: Maximum power point tracking (MPPT), One cycle control (OCC), Bidirectional ac to dc converter, PV Array, Proton exchange membrane fuel cell(PEMFC).

I. Introduction

A portion of huge gap between the expected demand and availability of the electricity produced in many parts of world, particularly in developing countries, is expected to be met from hybrid systems. A reliable and low-cost single phase grid connected inverter which requires little maintenance has become order of the day for interfacing such low- capacity systems to grid. Traditionally, diode rectifiers or thyristor bridge converters were employed to synthesize dc voltage from ac utility. These rectifiers pollute the utility with lower order harmonics, which are difficult to filter. Pulse width modulation (PWM) converters are employed to overcome this problem. These converters shift the frequency of the dominant harmonics to a higher value, so that they can be easily filtered by employing small passive filter [1]-[2]. The PWM bidirectional converter draws a near sinusoidal input current while providing a regulated dc voltage and can operate in the first and second quadrants of the voltage-current plane.

The configuration of single phase inverter based grid connected systems generally consists of two current control loops. A fast inner current controller regulates the current injected to the grid while maintaining prescribed total harmonic distortion (THD) and power factor, while slow outer current-control loop incorporates the MPPT algorithm employed. In order to interface the inverter with the grid, service of a phase locked loop (PLL) is required. Designing a phase locked loop for interfacing with a weak grid is always a difficult proposition considering the non idealities like frequency variation and harmonic distortions in the line voltages [12].more over the PLL routine consumes considerable computational resources of the digital image processor (DSP) employed for its realization. In an effort to simplify the control structure of grid-connected inverters in a pv systems based on one cycle control (OCC) have been proposed [4],[5]. Systems based on OCC do not require the service of a PLL [13]—[15]

A single phase OCC-based inverter for grid connected pv system which can operate at a maximum power point is represented in [5].the performance of this scheme is in tracking the maximum power from the solar array is very sensitive to the set of design parameters chosen for the realization of the controller .hence, maximum power point operation is not guaranteed if there are changes in operating conditions and /or drift in the value of control and system parameters due to ageing. In order to overcome the aforementioned limitation, the value of the control parameters are obtained in [9]. By using a multi objective optimization procedure which extracts the highest average power for a given insolation range. however, the scheme reported in [9]. Make the system operate closer but not at the point of maximum power operating point (MPOP) for the designed range of insolation. In order to address the aforementioned problem, a customized perturb and observe (P&O) method for tracking the maximum power point is applied to an OCC based scheme so that the system operates at the MPOP even if there is a variation in the isolation level and parameter values [4]. The controller of the scheme presented

in [4]. Needs to sense grid voltage ,grid current, DC link voltage. it also needs to sense the PV current to realize the MPPT algorithm.

II. Modelling of Hybrid PV-FC System

2.1 Modelling of PV Array System

The electric power generated by a photovoltaic array is fluctuating according to the illumination and the temperature. The building block of PV arrays is the PV cell, which is basically a P-N junction semiconductor that products current via the photovoltaic effect. PV arrays are constructed by placing numerous PV cells connected in series and in parallel. The most commonly used model of a PV cell is the one-diode equivalent circuit as shown in Fig.1.

The current voltage characteristic of a PV cell is derived as follow:

$$I = I_{ph} - I_D$$

$$I = I_{ph} - I_0 \left[\exp\left(\frac{q(U + R_s I)}{A k_B T} - 1\right) - \frac{U + R_s I}{R_{sh}} \right]$$

where: I_{ph} =photo current (A), I_D =diode current (A), I_0 =saturation current (A), A =the diode quality constant (when $T=28C$, $A= 28$), q =electronic charge ($1.6 * 10^9$ C), k_B =Boltzmann's gas constant ($1.38 * 10^23$), T =cell temperature, R_s =series resistance (U), R_{sh} =shunt resistance (U), I =cell current (A), U =cell voltage (V).

There are several parameters (I_{ph} , I_0 , R_s , R_{sh} , T , etc) which need to be determined before the I_eU relationship can be obtained. In this paper a mathematical model of relation between the power, output current and output voltage is given based on technical parameters, such as short-circuit current (I_{sc}), open-circuit voltage (U_{oc}), maximum power current (I_m) and maximum power voltage (U_m), which could reflect the output characteristic of the PV cells.

The novel models are presented as follow.

At Standard Test Conditions (STC) ($T =25C$, $S=1000$ W/m2), the current voltage characteristic of a PV cell can be modeled mathematically using below Equations

$$I = I_{sc} \left(1 - C_1 \left\{ \exp \left[\frac{U_o}{C_2 U_{oc}} \right] - 1 \right\} \right)$$

$$C_1 = \left(1 - \frac{I_m}{I_{sc}} \right) \exp \left(- \frac{U_m}{C_2 U_{oc}} \right)$$

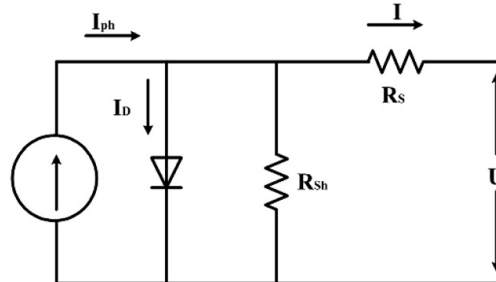


Fig. 1. One-diode equivalent circuit model of a PV cell.

$$C_2 = \left(\frac{U_m}{U_{oc}} - 1 \right) \left[\ln \left(1 - \frac{I_m}{I_{sc}} \right) \right]^{-1}$$

where: I_{sc} =short-circuit current (A), U_{oc} =open-circuit voltage (V), I_m =maximum power current (A), U_m = maximum power voltage (V), U_o =cell voltage (V), I =cell current (A).

According to the I_{sc} , U_{oc} , I_m , U_m on reference condition, the new parameters (I_{sc} , U_{oc} , I_m , U_m) can be developed, thus getting the new I_eU relationship considering the illumination intensity and temperature on the output characteristic of PV cell.

$$\begin{cases} \Delta T = T - T_{ref} \\ \Delta S = \frac{S}{S_{ref}} - 1 \\ I'_{sc} = I_{sc} \frac{S}{S_{ref}} (1 + a\Delta T) \\ U'_{oc} = U_{oc} (1 - c\Delta T) \ln(1 + b\Delta S) \\ I'_{m} = I_m \frac{S}{S_{ref}} (1 + a\Delta T) \\ U'_{m} = U_m (1 - c\Delta T) \ln(1 + b\Delta S) \end{cases}$$

2.2 Modelling of fuel cell

Hydrogen today is produced from natural gas from limited markets but it can be produced from renewable sources and promises substantial contributions to the global energy supplies in the long term. Hydrogen is most abundant element in the universe, the simplest chemical fuel (essentially a hydrocarbon without the carbon) that makes a highly efficient clean burning energy carrier. It has the potential to fuel transportation vehicle with zero emissions, provide process heat for industrial process, supply domestic heat through co-generation, help produce electricity from (centralized or distributed power systems and provide a storage medium for electricity from renewable sources. Sir William Grove (1811-96), a British lawyer and amateur Scientist, developed the first fuel cell in 1839. The principle was discovered by accident during an electrolysis experiment.

A fuel cell is an electrochemical device that converts chemical energy directly into electrical energy. Like a battery, a fuel cell consists of a pair of electrodes and an electrolyte. Unlike a battery, the species consumed during the electro chemical reactions are continuously replenished so that there is never a need to recharge the cell. A fuel visually hydrogen is supplied to the full cell anode. At the anode, the fuel is oxidized yielding electrons, which travel through the external circuit. At the Cathode, the oxidant is reduced, consuming electrons from the external circuit. Ions travel through the electrolyte to balance the flow of electrons through the external circuit. The anode and cathode reactions and the composition and direction of flow of the mobile ion vary with the type of fuel cell.

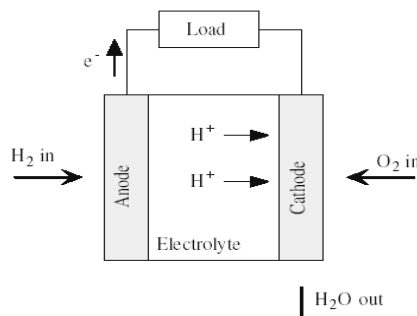


Fig.2. construction of typical fuel cell

III. One Cycle controlled Scheme

A single-stage grid-connected PV-FC system having a single phase full-bridge voltage source inverter is shown in Fig.3. The inverter switches are controlled to generate an output voltage from the inverter whose fundamental component is V_{I1} . By controlling the magnitude and phase of V_{I1} through a proper pulse width-modulation strategy, the power flow from the PV-FC to the grid can be controlled while maintaining a high power factor and low harmonic distortion.

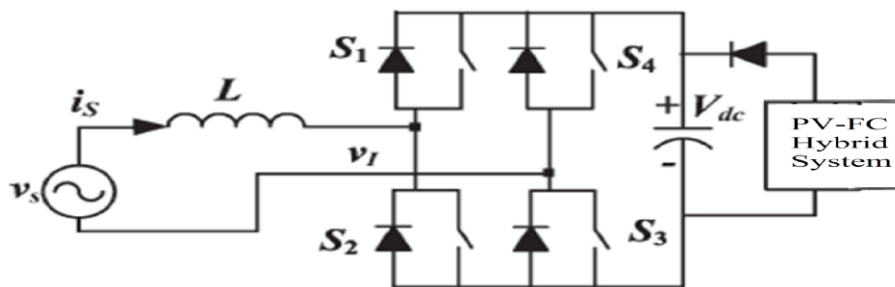


Fig.3.Single-phase grid-connected PV-FC system.

Basic OCC-based schemes exhibit instability in operation when the converter involved is operated in an inverting mode of operation. In order to overcome this problem, a modified OCC (M-OCC)- based scheme has been reported in [21]. Although the scheme presented in [21] does not require the service of a PLL, it needs to sense instantaneous grid voltage similar to the case of [4]. In the scheme reported in [21], the sensed grid voltage is multiplied by a constant gain to generate a fictitious current signal i_f in phase with the grid voltage. This fictitious current signal is then added to the actual current drawn by the inverter. The sum of these two signals is then used by the OCC core controller to generate gating pulses for the inverter switches.

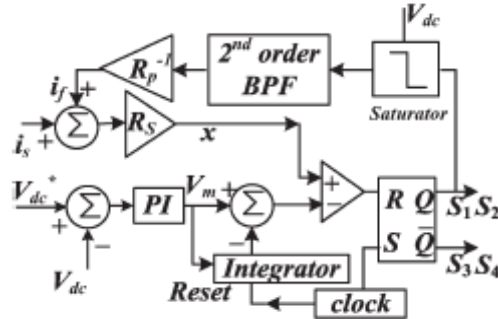


Fig.4. Control block diagram of the proposed OCC scheme.

The scheme proposed in this paper does not sense the grid voltage to generate the fictitious current signal required to circumvent the issue of instability in OCC-based inverter. It synthesizes the fictitious current signal required by multiplying the fundamental component of the inverter output voltage with a constant gain. Information regarding the inverter output voltage is obtained from the switching function used to trigger the inverter switches and not by sensing the inverter output voltage per se. The schematic control block diagram of the proposed scheme is shown in Fig. 4. The dc-link capacitor voltage is sensed and compared with a set reference, and the error so generated is fed to a proportional and integral regulator to produce a signal V_m . A sawtooth waveform of constant frequency having a peak-to-peak value of $2V_m$ is generated using a resettable integrator.

A free running clock having a time period T_s is used to reset the integrator, and hence, the frequency of the clock T_s^{-1} decides the frequency of the sawtooth waveform as well as the switching frequency of the device. Therefore, at steady state, when v_o is equal to V^* , the signal V_M is proportional to the real component of the source current of the converter. Using the signal V_M , a bipolar sawtooth waveform of amplitude V_M and having a time period of T_s is synthesized. This is achieved by integrating the signal V_M with a time constant T_i so that $T_i = T_s/2$

Where T_s is the time period of clock pulses, which resets the integrator. The switching frequency of the converter devices is the same as that of the frequency of the clock pulses. At every rising edge of the clock pulse, switches S_2 and S_4 are turned on, and the source (inductor) current increases. The expression for the rising slope $K1$ of the sensed source current signal is given as follows:

$$K1 = R_s ((v_s + V_o)/L) \tag{1}$$

Where v_s is the utility voltage, and L is the magnitude of the boost inductor. The output of the comparator, which compares the inductor current with the sawtooth waveform, determines the turnoff instant of S_2 and S_4 , and the turn-on instant of S_1 and S_3 . When S_1 and S_3 are turned on, the sensed boost inductor current signal falls with a slope $K2$. The value of the slope is given as follows:

$$K2 = R_s ((v_s - V_o)/L) \tag{2}$$

Fig.5 shows the logic used to generate the switching signals by comparing the sawtooth waveform with the source current, wherein d is the duty ratio of S_2 and S_4 . The control equation for the converter as given in [17] is presented as follows:

$$V_M(1 - 2d) = R_s i_s \tag{3}$$

It is also shown in [17] that the expression for the peak value of current in each switching cycle is

$$i_s = (V_M V_s) / (V_o R_s) \tag{4}$$

where R_s is the gain of the source current sensor. It can be inferred from (4) that the source current is proportional to the source voltage

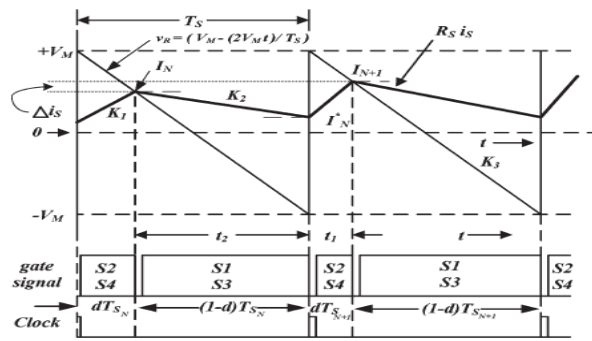


Fig.5. Source current along with the sawtooth waveform for the basic one-cycle-controller-based single-phase converter

The modulating signal x is being compared with the sawtooth waveform to generate the switching pulses. When x is less than the sawtooth waveform, S_1 and S_3 are on, and the output voltage of the inverter is $-V_{dc}$. when x is greater than the sawtooth waveform S_2 and S_4 are turned on, and the output voltage of the inverter $+V_{dc}$. Hence, the average output voltage of the inverter during a switching time period (time period of the sawtooth waveform) is

$$V_i = ((V_m - X) / 2V_m) (-V_{dc}) + ((V_m + X) / 2V_m) (V_{dc}) = (V_{dc} / V_m) X \quad (5)$$

IV. Modified OCC Scheme

The schematic control block diagram of the modified one cycle controller for the single-phase case is shown in Fig.6. A fictitious current, i_F , proportional to the source voltage V_S is generated by multiplying the sensed source voltage by a gain $1/R_F$. The signal $i_F R_S$ is then added to the sensed source current to obtain the signal $i_0 R_S$. The signal $i_0 R_S$ is then compared with the carrier sawtooth waveform to obtain the switching instants for the devices S_1 to S_4 . Therefore, in the modified one-cycle controller, instead of the signal $i_S R_S$, the signal $i_0 R_S$ is compared with the carrier sawtooth waveform, and the rest of the controller structure remains the same as that of the controller shown in Fig.4.

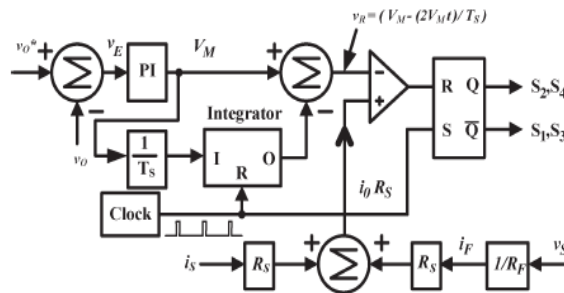


Fig.6 Control block diagram for the modified one cycle controller- based single phase converter.

The logic used to generate switching signals by comparing the sawtooth waveform with $R_S(i_S + i_F)$ is shown in Fig. 7. Hence, the control equations (3) and (4) get modified for the proposed controller as follows:

$$R_S(i_S + i_F) = V_M(1 - 2d) \quad (6)$$

$$i_S + i_F = (V_M V_S) / (V_O R_S) \quad (7)$$

or

$$V_S / R_e + V_S / R_f = (V_M V_S) / (V_O R_S) \quad (8)$$

Therefore

$$V_M = (R_S / R_e)(V_O) + (R_S / R_f)(V_O) \quad (9)$$

$$V_s < (LV_m / T_i * R_s) \tag{10}$$

Combining (9) and (10), the criterion for stable operation can be derived to be

$$1/R_f > T_i / (LV_o) V_s(\text{peak}) - 1/R_e \tag{11}$$

The system can be made to stably operate even when the converter is operating on no load ($R_e = \infty$) or when the converter is operating in the inverting mode ($R_e = -ve$).

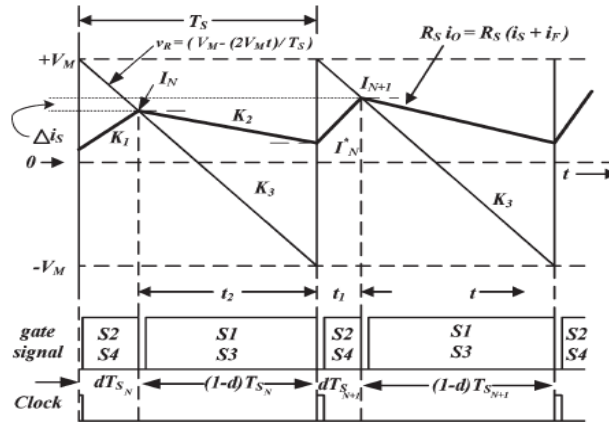


Fig.7. Source current and the fictitious current along with the sawtooth waveform for the proposed Modified one-cycle controller based single phase converter.

V. MPPT Implementation using P&O Method

P&O method is one of the popular methods to track the maximum-power point. Implementation of MPPT by P&O method is generally done by using DSP or microcomputer, but discrete analog and digital circuitry can also be used for the purpose [21]. The analog controller proposed in this paper for the implementation of the P&O algorithm is shown in Fig. 8.

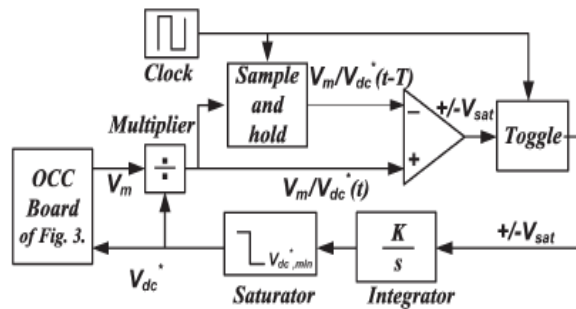
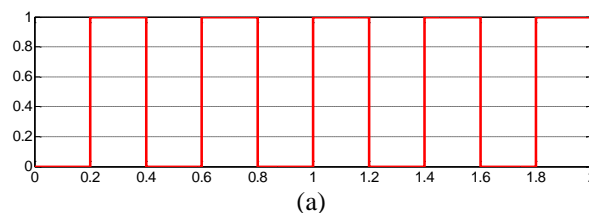


Fig. 8. Block diagram of the MPPT realization

The controller consists of an analog multiplier, a sample and hold circuit, a free-running clock, a toggle switch, and an integrator. The P&O controller receives the signal V_m from the OCC controller of Fig. 4. The output of the P&O controller is V_{dc}^* which sets dc-link voltage reference required by the OCC controller of Fig. 5. An integrator connected to the output of a toggle flip-flop generates the voltage reference V_{dc}^* . The period of the P&O cycle is decided by a free-running clock which sets sampling instants for the sample-and-hold circuit and toggling instants for the toggle flip-flop. In order to understand the working of the MPPT controller, the typical variations of the different signals of the MPPT controller block are shown in Fig. 9.



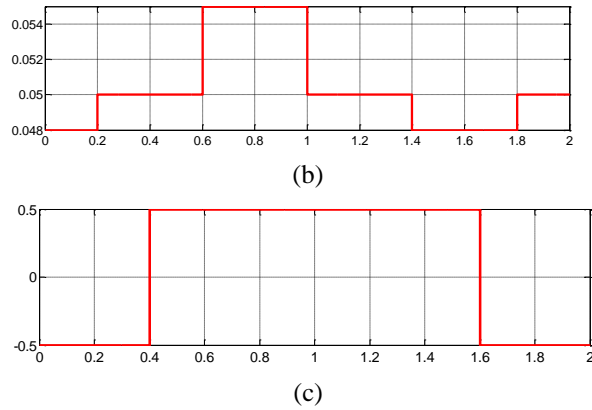


Fig.9. Typical variations of the various signals of the MPPT block. (a) MPPT clock. (b) sample-and-hold output. (c) Output of toggle flip-flop.

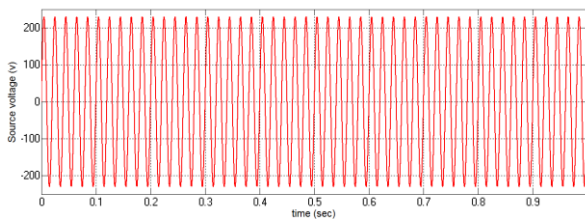
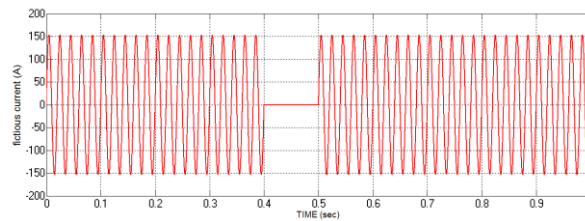
VI. Simulation Results

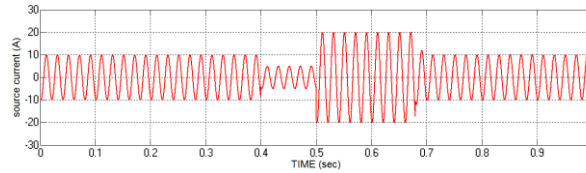
In order to predict the performance of the proposed modified one cycle-controlled grid-connected PV-FC system, detailed simulation studies are carried out on MATLAB–Simulink platform. In order to objectively show that the proposed voltage-sensorless scheme does not have the problem of current in stability while operating in the inverting mode of operation, a model of the system shown in Fig.10 is simulated. The specifications for the solar array used in the simulation study, corresponding to two different insolation levels (1000 and 500 W/m²), are provided in Table I. The insolation level considered for this simulation is 1000 W/m², and the dc-link reference is externally set at 560 V. The grid considered is a 230-V-rms50-Hz system. The parameters of the inverter chosen for the purpose of simulation and the controller are as follows:

- 1) switching frequency: 20 kHz;
- 2) dc-link capacitor: 2200 μ F;
- 3) series inductor: 2 mH;
- 4) R_p : 1.5 Ω ;

Table I
PV Array Specifications

Peak power (P_p)	2 kW	0.98kW
Peak power voltage (V_{mp})	560 V	540 V
Current at peak power (I_{mp})	3.5 A	1.8 A
Short circuit current (I_{sc})	3.9 A	2.1 A
Open circuit voltage (V_{oc})	700.0 V	680.0 V
Solar insolation	1000 W/m ²	500 W/m ²



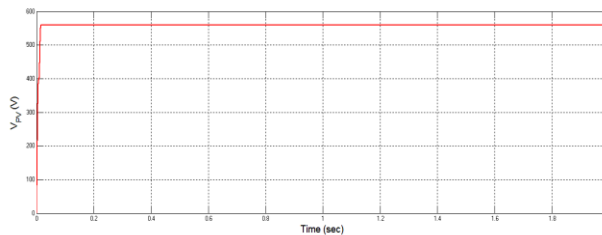


(c)

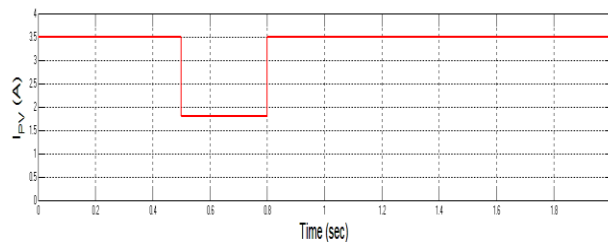
Fig.10. Simulated performance depicting the stable operation of the proposed scheme.

- a) Fictitious current
- b) Grid voltage
- c) Grid current

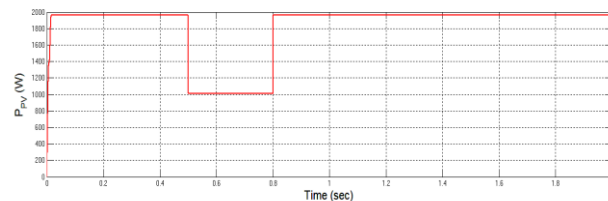
A simulated performance of the OCC-based voltage sensorless scheme showing the effectiveness of the fictitious current signal if in stabilizing the system is demonstrated in Fig. 10. The fictitious current if is made equal to zero at 0.4s and restored back again at 0.5 s. During the period from 0.4s to 0.5 s, when if is equal to zero, the system operates as a conventional OCC-based system trying to operate in the inverting mode. It can be observed from Fig. 10 that the system has become unstable during this period as dc-link voltage has become uncontrollable and the signal V_m assumes a negative value. At 0.5 s when if is restored back, operation of the system has become stable, and the signal V_m assumes a positive value. As the grid voltage and source current are almost 180° out of phase, the scheme is supplying power to the grid at a very high power factor. From this simulated behavior, it can be inferred that the dynamic response of the proposed MOCC based voltage-sensorless system is quite fast, and no instability in current controllability is observed during the inverting mode of operation. A sampling period of 0.4 s is used for the P&O algorithm used for realizing the MPPT



(a)



(b)



(c)

Fig.10. PV Array outputs a) PV Voltage b) PV Current c) PV Power

Due to disadvantage of PV energy is that the PV output power depends on weather conditions and cell temperature, making it an uncontrollable source. Furthermore, it is not available during the night. In order to overcome these inherent drawbacks, alternative sources, such as PEMFC, should be installed in the hybrid system. We are consider irradiance at 1.5 sec is zero therefore the pv array voltage is zero. At that time, fuel cell voltage fulfill our demand. The simulation of PV-FC Hybrid system output voltage, current and power are shown in below Fig.11.

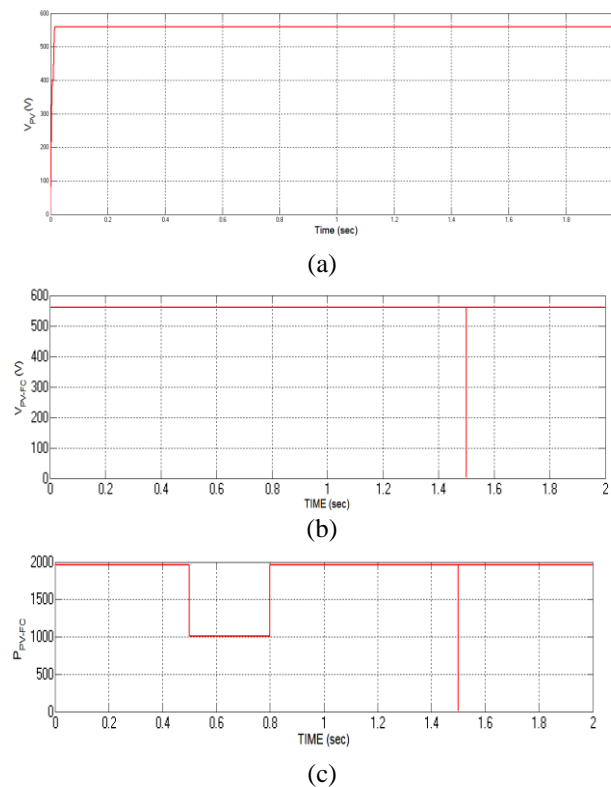


Fig.11. Simulation results of PV-FC Hybrid system a) FC Voltage b) PV-FC Voltage c) PV-FC Power

VII. Conclusion

An M-OCC-based single-phase grid connected PV-FC hybrid system has been proposed. The inherent limitation of the existing OCC-based inverters, such as the requirement for sensing the grid voltage to tackle the instability problem, is circumvented in the proposed scheme. The proposed scheme is based on a single stage of power conversion and is realized by utilizing a considerably less number of sensors compared to that of conventional schemes. Further, the core controller of the proposed scheme can be realized by means of a very simple analog controller. All the aforementioned features of the scheme make it an ideal candidate for small and distributed single-phase grid-connected PV-FC hybrid systems. Detailed simulation studies have been carried out to verify the effectiveness of the scheme.

References

- [1] B. T. Ooi, J. W. Dixon, A. B. Kulkarni, and M. Nishimoto, "An integrated AC drive system using a controlled current PWM rectifier/inverter link," *IEEE Trans. Power Electron.*, vol. 3, no. 1, pp. 64–70, Jan. 1988.
- [2] M. Calais, J. Myrzik, T. Spooner, and V. Agelidis, "Inverters for single-phase grid connected photovoltaic systems—An overview," in *Proc. IEEE Power Electron. Spec. Conf.*, Jun. 2002, pp. 1995–2000.
- [3] S. B. Kjaer, J. K. Pedersen, and F. Blaabjerg, "Power inverter topologies for photovoltaic modules—A review," in *Conf. Rec. IEEE IAS Annu. Meeting*, 2002, vol. 2, pp. 782–788.
- [4] M. Fortunato, A. Giustiniani, G. Petrone, G. Spagnuolo, and M. Vitelli, "Maximum power point tracking in a one cycle controlled single stage photovoltaic inverter," *IEEE Trans. Ind. Electron.*, vol. 55, no. 7, pp. 2684–2693, Jul. 2008.
- [5] Y. Chen and K. M. Smedley, "A cost-effective single-stage inverter with maximum power point tracking," *IEEE Trans. Power Electron.*, vol. 19, no. 5, pp. 1289–1294, Sep. 2004.
- [6] S. V. Araujo, P. Zacharias, and R. Mallwitz, "Highly efficient single-phase transformerless inverters for grid-connected photovoltaic systems," *IEEE Trans. Ind. Electron.*, vol. 57, no. 9, pp. 3118–3128, Sep. 2010.
- [7] T. Kerekes, R. Teodorescu, P. Rodriguez, G. Vazquez, and E. Aldabas, "A new high-efficiency single-phase transformerless PV inverter topology," *IEEE Trans. Ind. Electron.*, vol. 58, no. 1, pp. 184–191, Jan. 2011.
- [8] N. Femia, D. Granzio, G. Petrone, G. Spagnuolo, and M. Vitelli, "Optimized one cycle control in photovoltaic grid connected applications," *IEEE Trans. Aerosp. Electron. Syst.*, vol. 42, no. 3, pp. 954–972, Jul. 2006.
- [9] G. Petrone, G. Spagnuolo, and M. Vitelli, "A multivariable perturb-and-observe maximum power point tracking technique applied to a single stage photovoltaic inverter," *IEEE Trans. Ind. Electron.*, vol. 58, no. 1, pp. 76–84, Jan. 2011.
- [10] B. Sahan, A. N. Vergara, N. Henze, A. Engler, and P. Zacharias, "A single stage PV module integrated converter based on a low-power current source inverter," *IEEE Trans. Ind. Electron.*, vol. 55, no. 7, pp. 2602–2609, Jul. 2008.
- [11] F. Chan and H. Calleja, "Reliability estimation of three single-phase topologies in grid-connected PV systems," *IEEE Trans. Ind. Electron.*, vol. 58, no. 7, pp. 2683–2689, Jul. 2011.
- [12] S. Chattopadhyay and V. Ramanarayanan, "Digital implementation of a line current shaping algorithm for three phase high power factor boost rectifier without input voltage sensing," *IEEE Trans. Power Electron.*, vol. 19, no. 3, pp. 709–721, May 2004.

- [13] Q. Chongming and K. M. Smedley, "Unified constant-frequency integration control of three-phase standard bridge boost rectifiers with power factor correction," *IEEE Trans. Ind. Electron.*, vol. 50, no. 1, pp. 100–107, Feb. 2003.
- [14] K. M. Smedley, L. Zhou, and C. Qiao, "Unified constant-frequency integration control of active power filters—Steady-state and dynamics," *IEEE Trans. Power Electron.*, vol. 16, no. 3, pp. 428–436, May 2001.
- [15] K. Chatterjee, D. V. Ghodke, A. Chandra, and K. Al-Haddad, "Simple controller for STATCOM-based var generators," *IET Power Electron.*, vol. 2, no. 2, pp. 192–202, Mar. 2009.
- [16] N. Femia, M. Fortunato, G. Petrone, G. Spagnuolo, and M. Vitelli, "Dynamic model of a grid-connected photovoltaic inverter with one cycle control," in *Proc. 35th Annu. Conf. IEEE Ind. Electron.*, Nov. 2009, pp. 4561–4565.
- [17] Q. Chongming, K. M. Smedley, and F. Maddaleno, "Unified constant frequency integration control of active power filters—steady-state and dynamics," *IEEE Trans. Power Electron.*, vol. 16, no. 3, pp. 428–436, May 2001.
- [18] J. Alonso-Martinez, J. Eloy-Garcia, D. Santos-Martin, and S. Arnalte, "A new variable frequency optimal direct power control algorithm," *IEEE Trans. Ind. Electron.*, to be published.
- [19] I. Takahashi and Y. Ohmori, "High-performance direct torque control of an induction motor," *IEEE Trans. Ind. Appl.*, vol. 25, no. 2, pp. 257–264, Mar./Apr. 1989.
- [20] B. Han, S. Baek, and H. Kim, "New controller for single-phase PWM converter without AC source voltage sensor," *IEEE Trans. Power Del.*, vol. 20, no. 2, pp. 1453–1458, Apr. 2005.
- [21] D. V. Ghodke, K. Chatterjee, and B. G. Fernandes, "Modified one cycle controlled bi-directional high power factor AC to DC converter," *IEEE Trans. Ind. Electron.*, vol. 55, no. 6, pp. 2459–2472, Jun. 2008.



Sattineni Nagaprasad graduated from the Bhimavaram institute of engineering & technology, Andhra Pradesh, India, in 2011. His master of Technology in the Department of Electrical & Electronics Engineering, Swarnandhra Engineering College, Andhra Pradesh, India. His research interests include inverters, Renewable energy sources like pv, wind, fuel cell.



Boliseti Naveen graduated from the Bhimavaram institute of engineering & technology, Andhra Pradesh, India, in 2011. His master of engineering in the Department of Electrical & Electronics Engineering, SRKR Engineering College, Andhra Pradesh, India. His research interests include microgrids, distributed generation systems, power quality issues of electrical systems.



P. RAMPRASAD has received his B.Tech degree (EEE) from S.V.H. College of Engg & Tech in the year 2004. He has received his M.Tech degree from Karunya University with the specialization of Power Electronics & Drives in the year of 2009. His area of interest is Power Electronics, Industrial Drives.